Structural and electronic properties of NM-doped ceria (NM = Pt, Rh): a first-principles study

2008 J. Phys.: Condens. Matter 20 035210

(http://iopscience.iop.org/0953-8984/20/3/035210)

J. Phys.: Condens. Matter **20** (2008) 035210 (7pp) doi:10.1088/0953-8984/20/03/035210

Structural and electronic properties of NM-doped ceria (NM = Pt, Rh): a first-principles study

Zongxian Yang[1,4], Gaixia Luo[1], Zhansheng Lu[1], Tom K Woo[2] and Kersti Hermansson[3,4]

[1] College of Physics and Information Engineering, Henan Normal University, Xinxiang, Henan 453007, People's Republic of China
[2] Department of Chemistry, University of Ottawa, ON, K1N 6N5, Canada
[3] Materials Chemistry, The Ångström Laboratory, Uppsala University, Box 538, SE-75121, Uppsala, Sweden

E-mail: yzx@henannu.edu.cn and kersti.hermansson@mkem.uu.se

Received 8 June 2007, in final form 23 October 2007
Published 17 December 2007
Online at stacks.iop.org/JPhysCM/20/035210

Abstract
The effects of noble metal (NM) dopants (NM = Pt, Rh) on the structural and electronic properties of ceria are studied using a density functional theory (DFT) method, with the inclusion of on-site Coulomb interaction (DFT + U). It is found that these NM dopants give rise to large perturbations of the atomic and electronic structures of ceria and induce metal-induced gap states at the Fermi level suitable for accommodating extra electrons, thereby lowering the reduction energy of ceria and making the NM-doped cerias more reducible than pure ceria. This mechanism for facilitating the reduction of ceria is different from that of Zr-doped ceria where the increased reducibility is largely due to the structural distortions and not to electronic modifications.

(Some figures in this article are in colour only in the electronic version)

1. Introduction

In the past few decades, environmental protection has become an increasing worldwide concern. Automobile exhaust is a major cause of air pollution. Three-way catalysts (TWC) which can eliminate CO, HCs (hydrocarbons), and NO_x simultaneously have been used to control exhaust emissions for decades. A conventional TWC usually contains noble metal(s) (NM: Pd, Pt, and/or Rh) and CeO_2 on an Al_2O_3 support. A good deal of information is available in the literature for Pt/CeO_2 [1–10], Pd/CeO_2 [8, 11–17] and Rh/CeO_2 [1, 12, 18–24]. CeO_2 and related compounds have attracted much attention [6–8, 25–32] thanks to its favorable redox properties [33, 34]. An increase in the number and mobility of oxygen vacancies in ceria has been found to enhance its oxygen storage capacity as well as its catalytic activity [35].

Due to the large number of lattice defects, ceria can provide a large number of active sites for gas–solid catalysis, especially if doped with other metal atoms of lower oxidation state. Structurally, a dopant can introduce stress into the lattice of an oxide host, inducing in this way the formation of defects to fulfill charge neutrality and modifying the chemical reactivity. On the other hand, the oxide host lattice can impose nontypical coordination structures for the dopant with subsequent perturbation of the dopant's chemical properties. For all these reasons, it is important to gain a better understanding of the behavior of metal-doped CeO_2.

Some experimental results [8, 32, 36] have given indications of NM diffusion into the ceria support. Bernal *et al* [8] suggested that metal decoration phenomena occur on the three NM/CeO_2 catalysts. Zhou *et al* [20] suggested the migration of Rh into ceria to form a strong metal oxide interaction. Imamura *et al* [32] showed that Pt interacts very strongly with ceria, indicating the possibility of the formation of Pt–O–Ce bonds and the penetration of Pt into the bulk ceria.

[4] Authors to whom any correspondence should be addressed.

The combination of Pt with CeO_2 has been found to make the TWC highly active for the oxidation of CO and H_2. Sun *et al* [36] reported the observation that Pd particles sank into the ceria–zirconia support after reduction.

Besides our recent paper dealing with a Pd dopant in ceria [37], we are not aware of any other electronic structure calculations of NM-doped ceria in the literature and the effects of NM diffusion as dopants into the ceria support are not clear yet. Although surface properties are also highly relevant to the redox properties of ceria and ceria-based materials, and have been studied theoretically [38–40], in this paper, we present first-principles study on the Pt, Rh-doped bulk ceria and focus on the effects of Pt, Rh dopants on the properties of ceria.

2. Methodology

There are different theoretical approaches used for modeling defects in solids, including 'the periodic supercell approach', 'the cluster in Vacuo' and 'the embedded cluster' models, etc [41, 42], and references therein. In the present paper we use the periodic supercell approach, which has become quite a standard and popular method in modeling defects and surfaces. For all calculations reported in this paper, we have used a large 96-atom supercell, i.e. a $2 \times 2 \times 2$ supercell built from the conventional 12-atom cubic unit cell of CeO_2 to reduce the dopant–dopant and the vacancy–vacancy interactions that are a consequence of the periodic boundary conditions. Very recently, this kind of supercell has been successfully used to study reduced ceria [25] and ceria with dopants [37, 43, 44]. The dopant–dopant and the vacancy–vacancy distances in our 96-atom cell are as large as about 10.96 Å. As will be seen in the results section, the atomic structural and electronic perturbation from the dopant and vacancy are found to be quite localized around the dopant and vacancy centers and the calculated vacancy formations energies are found to be converged with this separation. The supercell we use thus appears quite reasonable to model the NM-doped ceria.

The NM-doped ceria was modeled by introducing one NM dopant atom to substitute one Ce atom in the supercell, corresponding to a dopant concentration of 3%. The doped systems were assumed to keep the cubic structure, while the cell parameter and atomic positions were optimized.

Starting from the relaxed pure and the NM-doped structures, oxygen vacancies were introduced by removing one of the oxygen atoms from the supercells. The systems were then allowed to relax again with the lattice parameter fixed. For the pure ceria, the position of the vacancy is unique, while for the doped ceria, there are different possible sites to create a vacancy in the supercell. Our previous paper [43] using a similar model for the Zr-doped ceria found that the vacancy is preferred to be created at the nearest neighbor (NN) site of the dopant. Test calculations for the present systems also show the same trend. Here, we have in all cases placed the oxygen vacancy at the NN site of the dopant.

For all the systems, spin-polarized calculations were performed using the first-principles density functional theory within the projector augmented wave (PAW) method [45, 46] as implemented in the *Vienna Ab initio Simulation Package* (VASP) [46, 47]. The Perdew–Burke–Ernzerhof (PBE) functional [48] was used for the exchange correlation. Recently, it was shown that conventional generalized gradient approximation (GGA) DFT calculations fail to give the correct electronic structure for reduced ceria [17, 39, 43]. However, the DFT + U method [49, 50] is able to reproduce the general features of the atomic and electronic structure of reduced ceria [25, 37, 39, 40, 43, 51, 52]. In the DFT + U method, a Hubbard parameter U is introduced for the Ce 4f electrons to describe the on-site Coulomb interaction; this helps to remove the self-interaction error and improves the description of correlation effects. It has been shown that by choosing an appropriate U parameter to account for the strong on-site Coulomb repulsion among the localized Ce 4f electrons, it is possible to consistently describe structural, thermodynamic, and electronic properties of CeO_2, Ce_2O_3, and CeO_{2-x}, which enables modeling of redox processes involving ceria-based materials [25]. Recently, Da Silva *et al* [26] applied hybrid functionals to the rare-earth oxides (including ceria) and correctly predicted Ce_2O_3 to be an insulator as opposed to the ferromagnetic metal predicted by the local spin density (LDA) and generalized gradient (GGA) approximations. This shows another possibility of using hybrid functionals (other than the DFT + U method used here) to reduce the improper self-interaction. In this paper, the DFT + U method [49, 50] is used. We have chosen a value of 5 eV for the U parameter for all calculations presented herein. This is in agreement with the value suggested by [25, 39, 40], which suggested that for $U \geqslant 5$ eV, the electronic structure was essentially converged.

In our calculations, the Ce 5s5p5d4f6s, O 2s2p, Pt 5d6s, and Rh 4d5s are treated as valence electrons. An energy cutoff of 30 Ryd was used for the plane wave expansion of the PAWs. The Monkhorst–Pack (MP) method was used for Brillouin Zone sampling [53]. A MP grid of $(2 \times 2 \times 2)$ was used for the 96-atom cells. For all structures, the ionic positions were allowed to relax until the Hellmann–Feynman forces were less than 0.02 eV $Å^{-1}$. These values have been found to give good convergence of all quantities under consideration in the present study.

3. Results and discussion

3.1. Structural properties

Our calculated undoped CeO_2 bulk supercell has an optimized lattice constant of 10.960 Å, which corresponds to a unit cell lattice constant of 5.480 Å. The experimental value is 5.411 Å [54]. Upon doping with one Pt or Rh atom, the relaxed supercell shows a very small decrease in the lattice constants. The optimized lattice constant is 10.95 Å for Pt-doped CeO_2 supercell and 10.94 Å for Rh-doped CeO_2 supercell. The smaller ionic radii of Pt^{2+} (0.86 Å) and Rh^{3+} (0.75 Å) as compared to the Ce^{4+} radius (0.97 Å) essentially explain the decrease in the cell parameters.

It should be stressed that our periodic supercell model for NM-doped ceria corresponds to solid solutions of the type $Ce_{0.97}NM_{0.03}O_{2-x}$ with a homogeneous distribution of dopant ions and oxygen vacancies, rather than an isolated defect

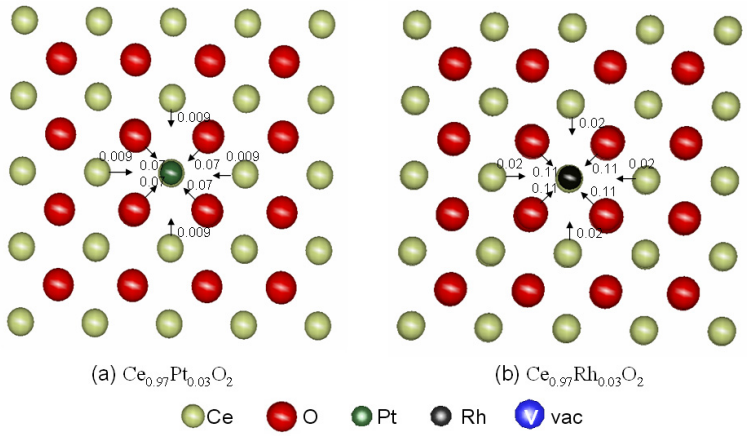

Figure 1. The relaxed structure for the unreduced systems: (a) $Ce_{0.97}Pt_{0.03}O_2$, and (b) $Ce_{0.97}Rh_{0.03}O_2$. Here and in the following figures, yellow, purple, red, green and black spheres represent the Ce^{4+}, Ce^{3+}, O, Pt and Rh ions, respectively. The blue sphere shows the position of a vacancy.

using the cluster models [41, 42]. The large supercell we use effectively reduces dopant–dopant and vacancy–vacancy interactions, as mentioned above.

For the unreduced, doped systems, the displacements of the ions around the dopants are shown in figure 1. The metal-induced displacements for the oxygen anions are about 0.07 Å and 0.11 Å; and the displacement for the cerium cations about 0.009 Å and 0.02 Å for the Pt- and Rh-doped ceria systems, respectively. We can see that in the unreduced systems, the Rh dopant causes a larger perturbation to the structure than the Pt dopant. The larger structural perturbation caused by Rh doping as compared to Pt doping can be explained by the smaller ionic radii of Rh as compared to Pt and Ce (0.97 Å for Ce^{4+}, 0.86 Å for Pt^{2+} and 0.75 Å for Rh^{3+}).

For the reduced systems, the displacements of the ions around the oxygen vacancy for the undoped and doped systems are shown in figure 2. The vacancy induces a nonsymmetric structural relaxation for undoped ceria (shown in figure 2(a)) which is essentially the same as our published results in [43]. The nearest neighbors of the vacancy are two Ce^{4+} ions and two Ce^{3+} ions. Thus all cerium ions neighboring the effectively 'positive' vacancy site move outwards by 0.14–0.18 Å, and some of the vacancy's next nearest neighbor (NNN) oxygen atoms move inwards (namely those with at least one Ce^{4+} neighbor; they move by 0.12 and 0.27 Å) while others move outwards (namely those with two Ce^{3+} neighbors, which move outwards by 0.04 Å). The vacancy-induced displacements shown in figures 2(b) and (c) for the NM-doped systems with an O vacancy located next to the NM dopant reveal relaxation patterns that are distinct from that of the undoped systems. Specifically, all nearest neighbor (NN) Ce cations move away (by about up to 0.16 and 0.15 Å for Pt- and Rh-doped systems, respectively) while the Pt and Rh dopant cations move toward the center of the vacancy (by 0.08 Å). The next nearest neighbor O anions move toward the center of the vacancy, with the two O anions that are close to the dopants having larger movement (by about 0.36 and 0.23 Å for Pt- and Rh-doped systems, respectively). The vacancy-induced displacements (of the oxygen anions) in the NM-doped systems have been perturbed more than those in the undoped system. The perturbation patterns also show that Pt has a more pronounced effect than Rh for the reduced systems. These differences are also reflected in the electron localization patterns which will be discussed in section 3.3.

The ions in the vicinity of the 'NM dopant–O vacancy' pair are strongly perturbed compared to the partially reduced undoped system. Moreover, the perturbation is larger for the Pt-doped system than for the Rh-doped system. This can be rationalized from the formal charges of the metal ions and the resulting changes in the local electric field next to the vacancy,with and without the presence of the NM dopants. Pt is nominally in a 2+ state compared to a 4+ state for Ce, whereas Rh is in a 3+ state in the doped and reduced ceria systems. As discussed in [43], large perturbations to the structure may be also rationalized in terms of the changes in the ionic sizes of Ce^{4+} and Ce^{3+} associated with the reduction. In NM-doped ceria, the ionic radii of the NM dopants (0.86 Å for Pt^{2+} and 0.75 Å for Rh^{3+}) are smaller than that of Ce^{4+} (0.97 Å, eight coordinated [55]). It is the combined effects of the electric field and the difference in atomic sizes that results in the structural rearrangement, where the Ce cations move away from the vacancy, while the NM dopants (Pt and Rh) and the O anions are attracted to it. One may expect that such a large structural perturbation induced by the NM dopant will have large effect on the redox properties of ceria. This will be discussed in the next section.

3.2. O vacancy formation energies

As mentioned in the introduction, doping may lead to an increase in the ability of CeO_2 to take up and release oxygen. The formation of a $Ce_{0.97}NM_{0.03}O_2$ solid solution by doping Pt^{2+}, Rh^{3+} ions into a CeO_2 lattice would generate even more oxygen vacancies due to charge balance requirements, resulting in more favorable redox properties and oxygen storage capacity. The O vacancy formation energy (E_{vac}) can be calculated from

$$E_{vac} = E(\text{Cell}_{vac}) + 1/2E(O_2) - E(\text{Cell}) \qquad (1)$$

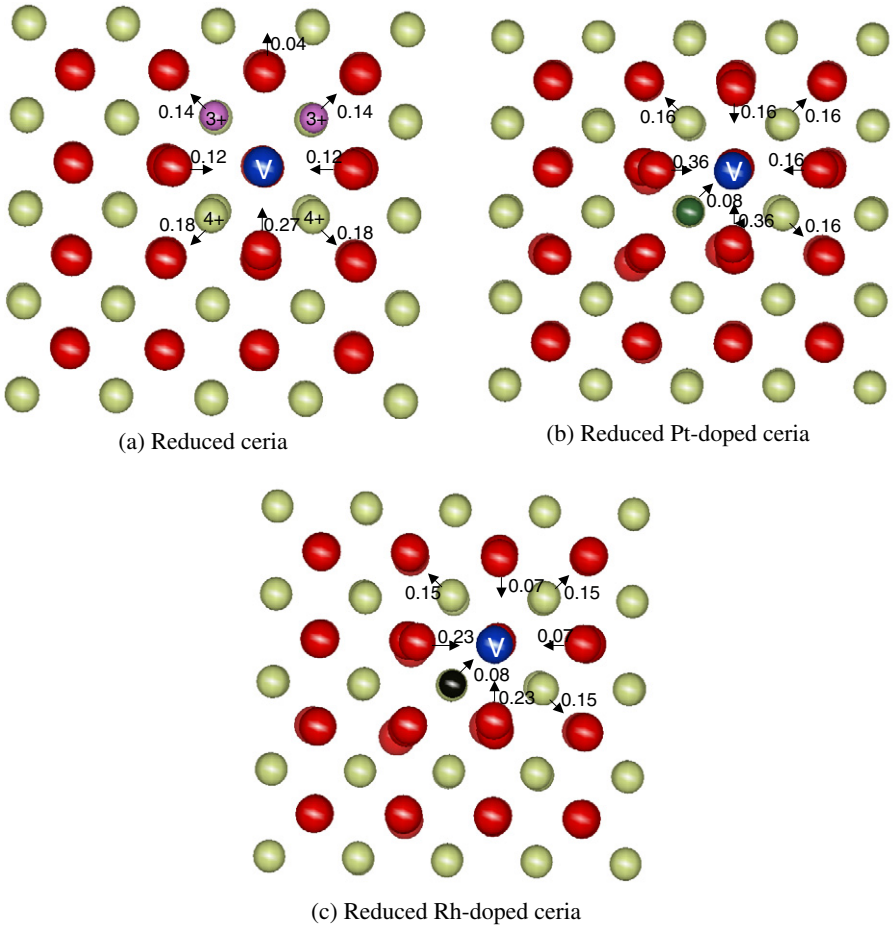

(a) Reduced ceria

(b) Reduced Pt-doped ceria

(c) Reduced Rh-doped ceria

Figure 2. The relaxation caused by the O vacancy. The spheres show the atomic positions in the relaxed reduced systems: (a) ceria, (b) Pt-doped ceria, and (c) Rh-doped ceria.

where $E(\text{Cell}_{\text{vac}})$ and $E(\text{Cell})$ are the total energies of the optimized supercells with and without an O vacancy, and $E(O_2)$ is the total energy for the ground state of an optimized oxygen molecule in the gas phase (calculated with the same supercell size and method as the solids). A positive value for E_{vac} means that energy is needed to create an O vacancy and the lower the value is, the easier it is to create a vacancy.

The calculated value of E_{vac} for the undoped ceria system is 2.99 eV per vacancy which is in agreement with [43], and the O vacancy formation energies are 0.96 eV and 1.37 eV for the Pt- and Rh-doped systems, respectively. Thus, the dopants lower the reduction energy by as much as 2.03 eV (for the Pt dopant) and 1.62 eV (for the Rh dopant), which shows that it is easier to reduce NM-doped ceria than pure ceria and suggests the possibility of increasing the oxygen storage capacity by dissolving NM into ceria. We find that Pt-doped ceria is easier to form O vacancies than Rh-doped ceria. This may explain the experimental observation [32] that the combination of Pt with CeO_2 makes the TWC highly active in the oxidation of CO and H_2.

Our vacancy formation energy results are consistent with the analysis of the variation in the displacements of the ions around the oxygen vacancy as discussed above, and with the details of the electronic structure of reduced NM-doped cerias as given below.

The mechanism for the large reduction in the vacancy formation energy can partly be explained by simple electrostatic arguments. The Pt^{2+} and Rh^{3+} dopants are lower in formal charge than Ce^{4+}, and it is easier to form an oxygen vacancy from next to Pt^{2+} than next to Rh^{3+} than next to Ce^{4+}. On the other hand, the reduction in the vacancy formation energy can also be explained by the modifications of the electronic structure as induced by the NM dopants; this will be discussed in the following section.

3.3. The electronic properties

Since NM doping has such a large effect on the properties of ceria, it is essential to understand the mechanism. To this end, we have analyzed the electronic structure of doped and undoped, with and without O vacancies. In particular, the total density of states (TDOS) (figures 3 and 4), spin charge density distribution (figure 5) and partial electron density distribution (figure 6) will be discussed.

Figure 3(a) shows the TDOS for the unreduced ceria which shows that undoped CeO_2 is an insulator. The valence band has mostly O 2p character with some contribution from Ce 4f5d. The sharp peak in the gap is from the Ce 4f states and the states (not shown) above the empty Ce 4f states are due to Ce 5d and 6s. The TDOS for the NM-doped unreduced

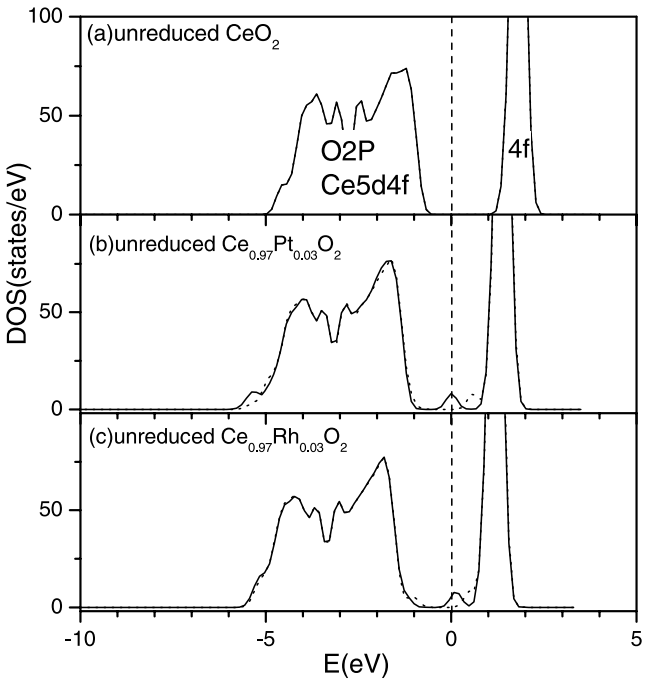

Figure 3. Total density of states (TDOS) for the unreduced systems: (a) ceria, (b) Pt-doped ceria, and (c) Rh-doped ceria. Here and in figure 4, both the DOSs for the majority spin (solid lines) and minority spin (dotted lines) are shown. The vertical dashed line at $E = 0$ eV represents the Fermi energy.

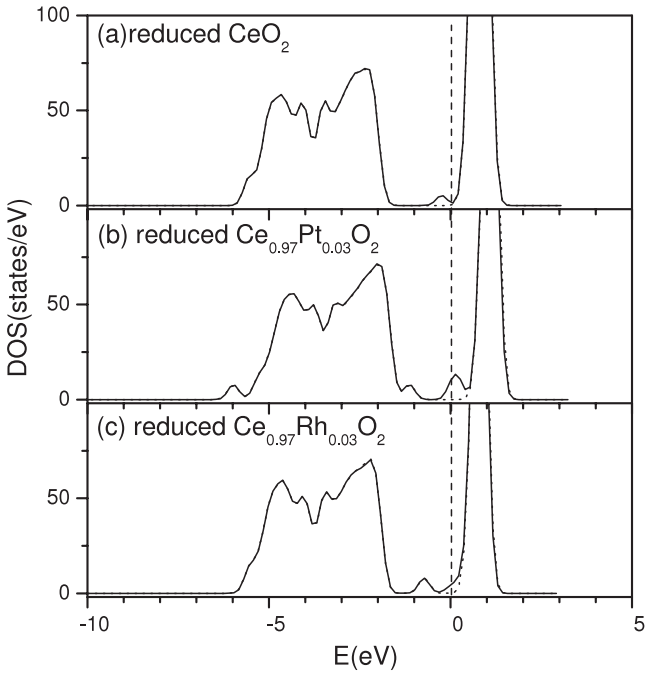

Figure 4. Total density of states (TDOS) for reduced systems: (a) ceria, (b) Pt-doped ceria, and (c) Rh-doped ceria.

ceria shown in figures 3(b) and (c), by contrast, is obviously affected by the doping. It shows that a feature corresponding to the metal-induced gap states (MIGS) appears below the empty Ce 4f states and the Fermi level is pinned in the gap states. By analyzing the partial density of states (PDOS) for the NM-doped unreduced ceria, we find that the MIGS are composed mainly of Pt 5d (Rh 4d) and O 2p states. From the spin charge density of the NM-doped ceria in figure 5, we are able to identify where the net spin resides. It is mainly localized on the dopants and their NN oxygen anions, residing in NM–O bonding (solid lines) and antibonding (dotted lines) states, with large Pt 5d (Rh 4d) and O 2p contributions. Thus, the MIGS are the result of the NM–O bonding. It is these partially occupied MIGS, as shown in figures 3(b) and (c), that potentially offer states suitable for accommodating extra electrons and therefore make the reduction easier. Indeed, we find that the MIGS acquire electrons left by the removed oxygen upon reduction, leading to a large reduction in the O vacancy formation energies in the NM-doped cerias as compared with the nondoped ceria. Comparing Pt- and Rh-doped ceria, we find that Pt doping results in a MIGS peak with higher DOS intensity at the Fermi level than does Rh doping, consistent with the different activities of the two NM-doped cerias.

In principle, there are a number of ways a dopant can increase the activity of an oxide and for the Pt/Rh-doped

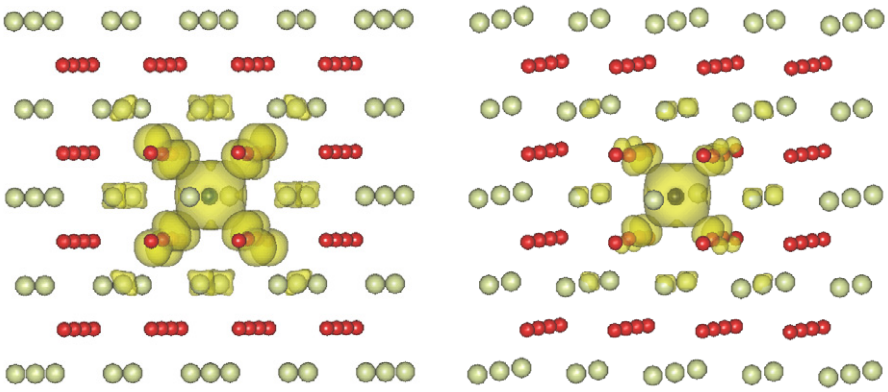

(a) Unreduced Pt-doped ceria (b) Unreduced Rh-doped ceria

Figure 5. The spin charge density ($\rho_a - \rho_b$) distributions for the unreduced systems: (a) Pt-doped ceria, and (b) Rh-doped ceria. The isosurface value used is 0.01 e Å^{-3}.

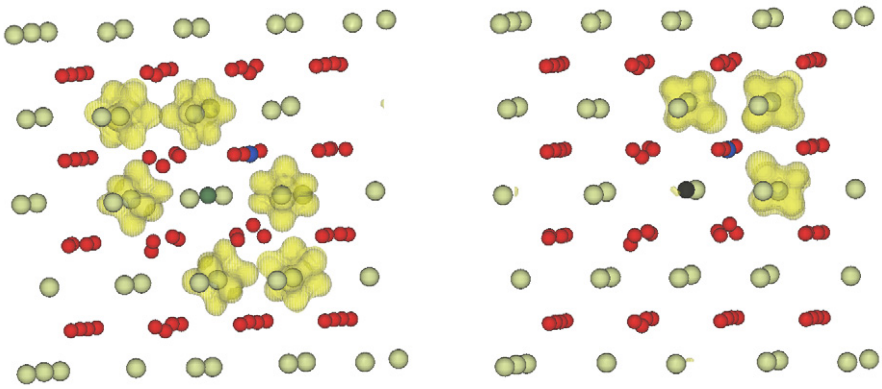

(a) Reduced Pt-doped ceria (b) Reduced Rh-doped ceria

Figure 6. The partial electron density distributions that correspond to the new gap states at the Fermi level (in the energy range from −0.4 to 0 eV as shown in figures 4(b) and (c)) for the reduced NM-doped ceria: (a) Pt-doped ceria, (b) Rh-doped ceria. The isosurface value used is 0.01 e $Å^{-3}$.

ceria systems we observe several. Electronic states from the metal appear in the gap, resulting in the metal-induced gap states or MIGS. A Bader-type AIM analysis [56] give net charges of +1.48 for the Pt ions and +1.60 for the Rh ions, respectively, in the NM-doped ceria systems. We also observe large structural perturbations around the doping centers. As seen above, the differences in the electronic properties of the $Ce_{1-x}NM_xO_2$ systems as compared with the undoped system have a strong impact on the activity of these mixed oxides.

Figure 4(a) shows the TDOS for the reduced ceria: a new peak appears in the O 2p–Ce 4f gap, with the Fermi level located in the gap between this new peak and the empty Ce 4f band. As discussed in [43], the electrons that occupy the new gap states are exactly localized on two Ce cations neighboring the oxygen vacancy, making the two Ce^{4+} cations reduced to Ce^{3+}.

The TDOS for the O-deficient NM-doped ceria are shown in figures 4(b) and (c). Compared to unreduced NM-doped ceria, the MIGS features of the NM-doped cerias move directly below the Fermi level, which are obviously induced by the presence of the O vacancy. This is because the gap states (the mixed Pt 5d or Rh 4d with O 2p) acquire some of the electrons left by the removed oxygen. This confirms the conjecture that NM dopant offers states suitable for accommodating extra electrons. Figures 4(b) and (c) also show that a new peak appears in the MIGS–Ce 4f gap, with the Fermi level located in the new peak. This new peak is also induced by the formation of the oxygen vacancy and corresponds to the reduction of cerium cations close to the vacancy. By analyzing the PDOS for the reduced NM-doped ceria, it is found that, with the formation of an oxygen vacancy, the 4f states of the Ce NNNs of the oxygen vacancy acquire electrons in Pt-doped reduced ceria, while it is the 4f states of the Ce NNs of the oxygen vacancy which acquire electrons in the case of Rh-doped reduced ceria. By plotting the partial electron density (figure 6) that corresponds to the new gap states at the Fermi level of the reduced NM-doped ceria, we find that the partial electron density of the Pt-doped ceria is mainly localized on six Ce NNNs of the O vacancy, while for Rh-doped ceria the partial electron density is located on three Ce NNs of the O vacancy. Therefore, in the Pt and Rh-doped reduced ceria systems, the dopants and the Ce cations all offer states suitable for accommodating extra electrons, which makes the doped ceria more easily reducible.

Comparing with Zr-doped ceria [43], we observe that the NM dopant utilizes a different mechanism to lower the reduction energy. For Pt and Rh, both structural distortions and the electronic modification (e.g. the appearing of the MIGS) contribute. For Zr, on the other hand, there are no new MIGS, and the electronic modification is unimportant. Therefore, the effect on E_{vac} is smaller, and is largely due to the structural distortions and subtle differences between Ce–O and Zr–O bonding.

4. Conclusions

The effects of noble metal (Pt and Rh) dopants on the atomic structure, electron distribution and reduction properties of ceria are studied using the first-principles density functional theory (DFT) method, with the inclusion of on-site Coulomb interaction (DFT + U). It is found that (1) these NM dopants give rise to large perturbation of the ceria structure, and induce MIGS at the Fermi level suitable for accommodating extra electrons left on oxygen vacancy formation, and therefore lower the reduction energy of ceria; (2) upon reduction, in addition to the NM dopants, some cerium cations close to the vacancy are partially reduced; (3) the O anions in the vicinity of an NM doping center display larger displacements than O anions in undoped ceria; (4) the major reason why the effect of Pt and Rh dopants on the oxygen vacancy formation energy is different from that of a Zr dopant is largely the difference in their electronic structures. The structural distortions are the most important factor for the Zr-doped material while the electronic modification is unimportant. For the NM-doped cerias both effects matter, making ceria more easily reducible than both pure ceria and Zr-doped ceria. It is also found that Pt and Rh display differences as dopants in ceria, e.g. the O anion

relaxation in the vicinity of the Pt dopant is higher than in the vicinity of the Rh dopant and Pt has the larger effect in lowering the reduction energy of ceria.

Acknowledgments

This work was supported by the National Natural Science Foundation of China (Grant No. 10674042) and Henan Innovation Project for University Prominent Research Talents (HAIPURT: 2007KYCX004) of China and the Swedish Research Council (VR).

References

[1] Bernal S, Calvino J J, Cauqui M A, Perez Omil J A, Pintado J M and Rodriguez-Izquierdo J M 1998 *Appl. Catal.* B **16** 127
[2] Fornasiero P, Kaspar J, Montini T, Graziani M, Dal Santo V, Psaro R and Recchia S 2003 *J. Mol. Catal.* A **204/205** 683
[3] Gonzalez-Velasco J R, Gutierrez-Ortiz M A, Marc J L, Botas J A, Gonzalez-Marcos M P and Blanchard G 2003 *Ind. Eng. Chem. Res.* **42** 311
[4] Penner S, Rupprechter G, Sauer H, Su D S, Tessadri R, Podloucky R, Schlogl R and Hayek K 2003 *Vacuum* **71** 71
[5] Silvestre-Albero J, Rodriguez-Reinoso F and Sepulveda-Escribano A 2002 *J. Catal.* **210** 127
[6] Bernal S, Blanco G, Calvino J J, Lopez-Cartes C, Perez-Omil J A, Gatica J M, Stephan O and Colliex C 2001 *Catal. Lett.* **76** 131
[7] Bernal S, Botana F J, Calvino J J, Cauqui M A, Cifredo G A, Jobacho A, Pintado J M and Rodriguez-Izquierdo J M 1993 *J. Phys. Chem.* **97** 4118
[8] Bernal S, Calvino J J, Cauqui M A, Gatica J M, Larese C, Perez Omil J A and Pintado J M 1999 *Catal. Today* **50** 175
[9] Hardacre C, Roe G M and Lambert R M 1995 *Surf. Sci.* **326** 1
[10] Liu Y, Hayakawa T, Ishii T, Kumagai M, Yasuda H, Suzuki K, Hamakawa S and Murata K 2001 *Appl. Catal.* A **210** 301
[11] Bunluesin T, Gorte R J and Graham G W 1998 *Appl. Catal.* B **15** 107
[12] de Leitenburg C, Trovarelli A and Kaspar J 1997 *J. Catal.* **166** 98
[13] Bunluesin T, Gorte R J and Graham G W 1997 *Appl. Catal.* B **14** 105
[14] Jen H W, Graham G W, Chun W, McCabe R W, Cuif J P, Deutsch S E and Touret O 1999 *Catal. Today* **50** 309
[15] Shen W-J and Matsumura Y 2000 *J. Mol. Catal.* A **153** 165
[16] Yao H C and Yu Yao Y F 1984 *J. Catal.* **86** 254
[17] Fabris S, de Gironcoli S and Baroni S 2005 *Phys. Rev.* B **72** 237102
[18] Mullins D R and Zhou J 2005 *229th ACS National Meeting (San Diego, CA, March, 2005)* PHYS (Abstracts of Papers)
[19] Mullins D R 2004 *Surf. Sci.* **556** 159
[20] Zhou T, Nakashima M and White J M 1988 *J. Phys. Chem.* B **92** 812
[21] Nakatsuji T, Ruotoistenmaki J, Komppa V, Tanaka Y and Uekusa T 2002 *Appl. Catal.* B **38** 101
[22] Mullins D R and Overbury S H 2002 *Surf. Sci.* **511** L293
[23] Bunluesin T, Gorte R J and Graham G W 1998 *Appl. Catal.* B **15** 107
[24] Bernal S, Blanco G, Cauqui M A, Corchado P, Pintado J M and Rodriguez-Izquierdo J M 1997 *Chem. Commun. (Cambridge)* 1545
[25] Andersson D A, Simak S I, Johansson B, Abrikosov I A and Skorodumova N V 2007 *Phys. Rev.* B **75** 035109
[26] Da Silva J L F, Ganduglia-Pirovano M V, Sauer J, Bayer V and Kresse G 2007 *Phys. Rev.* B **75** 045121
[27] Abi-aad E, Bechara R, Grimblot J and Aboukais A 1993 *Chem. Mater.* **5** 793
[28] Badri A, Binet C and Lavalley J-C 1996 *J. Phys. Chem.* **100** 8363
[29] Balducci G, Islam M S, Kaspar J, Fornasiero P and Graziani M 2000 *Chem. Mater.* **12** 677
[30] Bazin P, Saur O, Lavalley J C, Le Govic A M and Blanchard G 1998 *Stud. Surf. Sci. Catal.* **116** 571
[31] Bekyarova E, Fornasiero P, Kaspar J and Graziani M 1998 *Catal. Today* **45** 179
[32] Imamura S, Higashihara T, Saito Y, Aritani H, Kanai H, Matsumura Y and Tsuda N 1999 *Catal. Today* **50** 369
[33] Nunan J G, Robota H J, Cohn M J and Bradley S A 1992 *J. Catal.* **133** 309
[34] Taylor K C 1984 *Automobile Catalytic Converters* (Berlin: Springer)
[35] Daturi M, Bion N, Saussey J, Lavalley J C, Hedouin C, Seguelong T and Blanchard G 2001 *Phys. Chem. Chem. Phys.* **3** 252
[36] Sun H P, Pan X P, Graham G W, Jen H-W, McCabe R W, Thevuthasan S and Peden C H F 2005 *Appl. Phys. Lett.* **87** 201915
[37] Yang Z, Luo G, Lu Z and Hermansson K 2007 *J. Chem. Phys.* **127** 074704
[38] Yang Z, Woo T K, Baudin M and Hermansson K 2004 *J. Chem. Phys.* **120** 7741
[39] Nolan M, Grigoleit S, Sayle D C, Parker S C and Watson G W 2005 *Surf. Sci.* **576** 217
[40] Nolan M, Parker S C and Watson G W 2005 *Surf. Sci.* **595** 223
[41] Mysovsky A S, Sushko P V, Mukhopadhyay S, Edwards A H and Shluger A L 2004 *Phys. Rev.* B **69** 085202
[42] Van Speybroeck V, Stevens F, Pauwels E, Vrielinck H, Callens F and Waroquier M 2006 *J. Phys. Chem.* B **110** 8213
[43] Yang Z, Woo T K and Hermansson K 2006 *J. Chem. Phys.* **124** 224704
[44] Andersson D A, Simak S I, Skorodumova N V, Abrikosov I A and Johansson B 2007 *Appl. Phys. Lett.* **90** 031909
[45] Bloechl P E 1994 *Phys. Rev.* B **50** 17953
[46] Kresse G and Furthmüller J 1996 *Phys. Rev.* B **54** 11169
[47] Kresse G and Joubert D 1999 *Phys. Rev.* B **59** 1758
[48] Perdew J P, Burke K and Ernzerhof M 1996 *Phys. Rev. Lett.* **77** 3865
[49] Anisimov V I, Zaanen J and Andersen O K 1991 *Phys. Rev.* B **44** 943
[50] Dudarev S L, Botton G A, Savrasov S Y, Humphreys C J and Sutton A P 1998 *Phys. Rev.* B **57** 1505
[51] Fabris S, Vicario G, Balducci G, de Gironcoli S and Baroni S 2005 *J. Phys. Chem.* B **109** 22860
[52] Loschen C, Carrasco J, Neyman K M and Illas F 2007 *Phys. Rev.* B **75** 035115
[53] Monkhorst H J and Pack J D 1976 *Phys. Rev.* B **13** 5188
[54] Eyring L 1979 *Handbook on the Physics and Chemistry of Rare Earths* (Amsterdam: North-Holland)
[55] Shannon R D 1976 *Acta Crystallogr.* A **32** 751
[56] Henkelman G, Arnaldsson A and Jónsson H 2006 *Comput. Mater. Sci.* **36** 254